Noninvasive and Continuous Blood Pressure Monitoring Using Wearable Body Sensor Networks

Hao Lin, *Northeastern University, China*

Wenyao Xu, *State University of New York*

Nan Guan, Dong Ji, and Yangjie Wei, *Northeastern University, China*

Wang Yi, *Uppsala University, Sweden*

Hypertension is a major health risk that influences quality of life. A smartphone-centric body sensor network can help measure pulse transit time and continuously monitor blood pressure.

I t's well known that chronic hypertension has a strong impact on people's health and daily lives. Data from the Framingham Heart Study suggests that even though most individuals are normotensive at age 55, the chance for them to eventually become hypertensive is 90 percent.[1] In 2012, a report from the World Health Organization found that one-third of adults have high blood pressure (BP) and that the cause of roughly half of all deaths is stroke and heart disease (www.who.int/mediacentre/news/releases/2012/world_health_statistics_20120516/en).

BP is the amount of force applied on the walls of the arteries when blood is forced throughout the body, making it one of the most interesting hemodynamic parameters for assessing cardiovascular status. BP varies continuously due to different factors such as physical activities, medication, and emotions.[2] Noninvasive measurements such as cuff-based methods provide discrete values of BP, but they're limited to certain clinical or home-based scenarios. Moving beyond the use of external machines requires an alternative approach that's similarly continuous and noninvasive. Pulse transit time (PTT) is how long it takes a pulse wave to travel from one arterial site to another,[3] and several studies have shown it to have an inverse linear correlation with BP. An acute rise in BP causes an increase in vascular tone, hence the arterial wall becomes stiffer, causing a shorter PTT.[3]

Despite a strong correlation between PTT and BP, state-of-the-art methods using the former to infer the latter are still imprecise. A crucial reason is that the relationship between BP and PTT can change dynamically

Related Work in Noninvasively Measuring Blood Pressure

Researchers have proved the validity of using a noninvasive method to measure blood pressure (BP) in various studies. Current noninvasive methods can be classified into two categories: intermittent and continuous measurement.

Intermittent measurement based on the cuff method uses two traditional techniques: auscultation and oscillometry. According to Matthew Ward and Jeremy Langton,[1] these systems include three key components: an inflatable cuff, a method to determine the point of systolic and diastolic pressure, and a method to measure those pressures. Most of us are familiar with how this works: the cuff is placed around the upper arm and inflated. When the pressure point is reached, blood flow is prevented by the arterial wall. For auscultation, a mercury sphygmomanometer measures cuff pressure, and a stethoscope can determine the sounds over the brachial artery distal to an upper arm cuff.[2] Oscillometry measures BP by detecting oscillations in the cuff pressure during cuff deflation, with values estimated by using an indirect empirical method. However, this method is easily influenced by motion.[2]

Continuous BP measurement methods include the volume-clamp, tonometry-based, and pulse transit time (PTT)-based methods. The volume-clamp method[3] measures finger arterial pressure through a finger cuff and an inflatable bladder in combination with an infrared plethysmograph. Plethysmograph (a volume-measuring device) consists of an infrared light source and detector: the infrared light is absorbed by the blood, and the pulsation of arterial diameter during a heartbeat causes a pulsation in the light detector signal. Although this method typically generates good measurement results, ambulatory characteristics make it unsuitable to be used reliably and comfortably.[2]

Another noninvasive continuous BP measurement method is based on tonometry systems, in which an array of sensors is pressed against the skin over an artery. Although appealing because of its capability of providing accurate recording of arterial waveforms, applanation tonometry suffers two main limitations: the tonometer's placement over the artery is highly critical (the difference between correct and incorrect placement is within fractions of millimeters), and the need for continuous precise sensor positioning means that it's highly sensitive to motion (subjects are required to remain absolutely still while measurements are performed).

The PTT or pulse wave velocity (PWV) has been shown to be the most useful and convenient indirect parameter to measure BP both continuously and noninvasively.[4,5] To model the relationship between BP and PTT, Federico Cattivelli and Harinath Garudadri[6] constructed a linear relation to estimate BP. Considering that BP is highly correlated with instantaneous heart rate (HR), accordingly, Mico Wong and colleagues[7] added HR to this linear relation in their work. Heiko Gesche and colleagues[8] calculated PWV using the ratio between height and PTT, modeling the relation between BP and PWV with a correction constant that yields accurate results for estimating systolic BP. Many devices have been developed to measure PTT—for example, Daniel Wagner and colleagues[9] developed a PTT measurement platform with a single-channel ECG board and a pulse oximeter board. Petr Zurek and colleagues[10] designed a system that measures different biosignals, including electrocardiogram (ECG) and plethysmogram (PPG) signals, and then sends them to amplifiers and analog-to-digital convertors connected to a PC. The signals are processed in Matlab to calculate PTT. Stefan Hey and colleagues[11] designed a modular hardware setup that monitors certain physiological parameters in a long-term, noninvasive way, with the signals collected and saved to a notebook or PC. However, none of these systems are suitable for pervasive BP monitoring.

References

1. M. Ward and J.A. Langton, "Blood Pressure Measurement," *Continuing Education in Anaesthesia, Critical Care & Pain*, vol. 7, no. 4, 2007, pp. 122–126.
2. P.M.P. da Silva, "A Pervasive System for Real-Time Blood Pressure Monitoring," master's thesis, Dept. of Eng., Univ. of Porto, 2013; http://paginas.fe.up.pt/~ee08234/dissertacao/index.html.
3. J. Allen, "Photoplethysmography and Its Application in Clinical Physiological Measurement," *Physiological Measurement*, vol. 28, no. 3, 2007; http://iopscience.iop.org/article/10.1088/0967-3334/28/3/R01/pdf.
4. Z. Marcinkevics et al., "Relationship between Arterial Pressure and Pulse Wave Velocity Using Photoplethysmography during the Post-Exercise Recovery Period," *Acta Univesitatis Latviensis: Biology*, 2009, vol. 753, pp. 59–68.
5. R. Shriram et al., "Continuous Cuffless Blood Pressure Monitoring Based on PTT," *Proc. Int'l Conf. Bioinformatics and Biomedical Technology*, 2010, pp. 51–55.
6. F.S. Cattivelli and H. Garudadri, "Noninvasive Cuffless Estimation of Blood Pressure from Pulse Arrival Time and Heart Rate with Adaptive Calibration," *Proc. 6th Int'l Workshop Wearable and Implantable Body Sensor Networks*, 2009, pp. 114–119.
7. M.Y.M. Wong, C.C.Y. Poon, and Y.T. Zhang, "An Evaluation of the Cuffless Blood Pressure Estimation Based on Pulse Transit Time Technique: A Half Year Study on Normotensive Subjects," *Cardiovascular Eng.*, vol. 9, no. 1, 2009, pp. 32–38.
8. H. Gesche et al., "Continuous Blood Pressure Measurement by Using the Pulse Transit Time: Comparison to a Cuff-Based Method," *European J. Applied Physiology*, vol. 112, no. 1, 2012, pp. 309–315.
9. D.R. Wagner et al., "Relationship between Pulse Transit Time and Blood Pressure Is Impaired in Patients with Chronic Heart Failure," *Clinical Research in Cardiology*, vol. 99, no. 10, 2010, pp. 657–664.
10. P. Zurek et al., "Continuous Noninvasive Blood Pressure Measurement by Near Infrared CCD Camera and Pulse Transmit Time Systems," *Proc. 2nd Int'l Conf. Computer Eng. and Applications*, 2010, pp. 449–453.
11. S. Hey et al., "Continuous Noninvasive Pulse Transit Time Measurement for Psycho-Physiological Stress Monitoring," *Proc. Int'l Conf. eHealth, Telemedicine, and Social Medicine*, 2009, pp. 113–116.
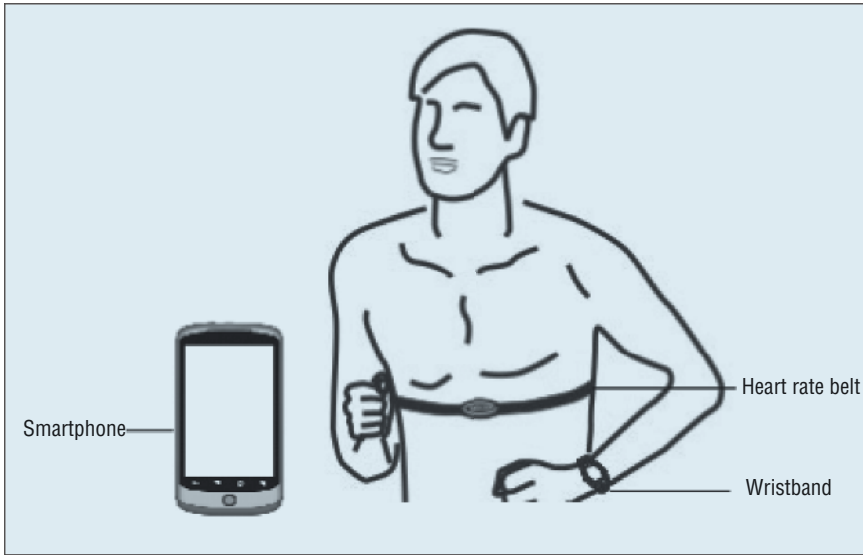
Figure 1. The system in use. The wristband is worn to collect plethysmogram (PPG) signals, and the heart rate (HR) belt is worn at the chest to collect electrocardiogram (ECG) signals. The wristband and the HR belt communicate with the smartphone via Bluetooth.
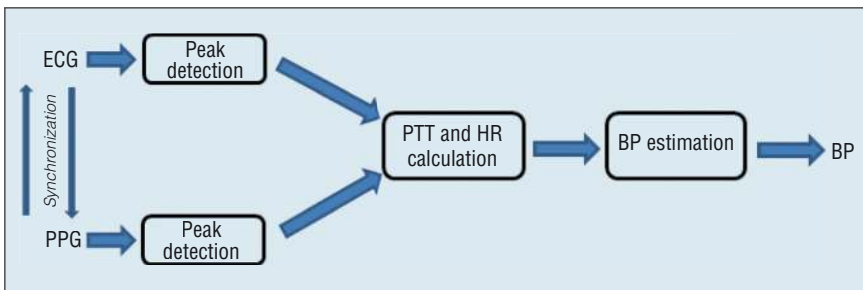

Figure 2. Analysis flow overview. ECG and PPG signals are transmitted to and processed on the smartphone.

due to other factors—for example, the correlation changes significantly before and after exercise.[4] A PTT calculation from an electrocardiogram (ECG) or plethysmogram (PPG) includes the pre-ejection period (PEP), making it longer than the true PTT[5] and indicating serious limitations for BP estimation from using only PTT. On the other hand, heart rate (HR) changes do have an influence on PTT changes.[6]

In this article, we propose a method that uses a body sensor network for continuous BP monitoring. BP values are calculated based on PTT that also consider baroreflex, which reflects the relationship between BP and HR. We evaluated our method with 300 sets of data from six subjects, and experimental results show that our proposed method can estimate the BP value in real time with a good precision more accurately than a state-of-the-art continuous BP monitoring method that uses only PTT. (See the related sidebar for others' work in this area.)

System Overview

Body sensor networks (BSNs) are widely used in medical health monitoring: they can be applied in a wearable device or used in a garment[7] to perform health monitoring flexibly and comfortably.

Our proposed BSN system estimates BP based on PTT, which is calculated from ECG and PPG signals. As Figure 1 shows, the BSN consists of three parts: wristband, HR belt, and smartphone. The wristband is worn as a wrist accessory to collect PPG signals, and the HR belt is worn at the chest to collect ECG signals. The wristband and the HR belt communicate with the smartphone via Bluetooth. As ECG and PPG signals are continuously collected and transmitted, an application on the smartphone can estimate PTT and BP. The user's BP is displayed on the smartphone or uploaded to servers.

Because PTT is calculated via ECG and PPG signals collected on different devices, synchronization between these two signal sources is important to achieve precision. ECG and PPG signals are transmitted to and processed on the smartphone; Figure 2 shows the smartphone's analysis flow.

Our system has great advantages in flexibility: BP is monitored without disturbing the subject's daily life. Monitoring continues no matter whether the subject is sitting at home or exercising outdoors.

Hardware Platform

Figure 3 shows the system architecture. The system consists of seven major components: two MSP430 microprocessor boards, two Bluetooth modules, an ECG module, a PPG module, and an analog-to-digital (A/D) converter. Subsystem 1 collects the ECG signal using an ECG module, and subsystem 2 collects the PPG signal from one finger. Each subsystem is controlled by a MSP430 microprocessor widely used in low-power electronics products. The sensor and Bluetooth modules are connected to MSP430 via its general I/O interfaces.

The ECG module uses the AD8232 single-lead ECG front end, and the PPG module is based on the SC0073 piezoelectric pressure sensor. The signals collected by the ECG and PPG sensors are digitized at 250 Hz by A/D converters. Figure 4 shows the two subsystems' hardware prototype.

The two subsystems are synchronized via their Bluetooth modules by transmitting a timestamp to each other; this process repeats after a fixed period. The sampled data are converted into digital signals and uploaded to the smartphone via Bluetooth. Figure 5 shows the collected ECG and PPG signals.

Signal Processing Chain for BP Estimation

To properly introduce our system, we must first look at its algorithm and software design.

Synchronization Protocol

A master-slave protocol synchronizes the clocks between the ECG and PPG subsystems. The ECG subsystem acts as the master, transmitting synchronization messages via Bluetooth to the PPG subsystem. The PPG subsystem receives the message and answers immediately. Finally, the ECG subsystem estimates the timing offset between the two subsystems. Figure 6 shows the procedure.

The connection between the two Bluetooth modules is established when the system starts to run. After a certain amount of time, the system is stable and the synchronization procedure starts. First, the master device records its timestamp as T_1 and transmits it to the slave device. As soon as the slave receives it, the slave stores its own timestamp as T_2 and sends back its timestamp to the master. The returned timestamp is recorded as T_3. When the master receives the message, it records its
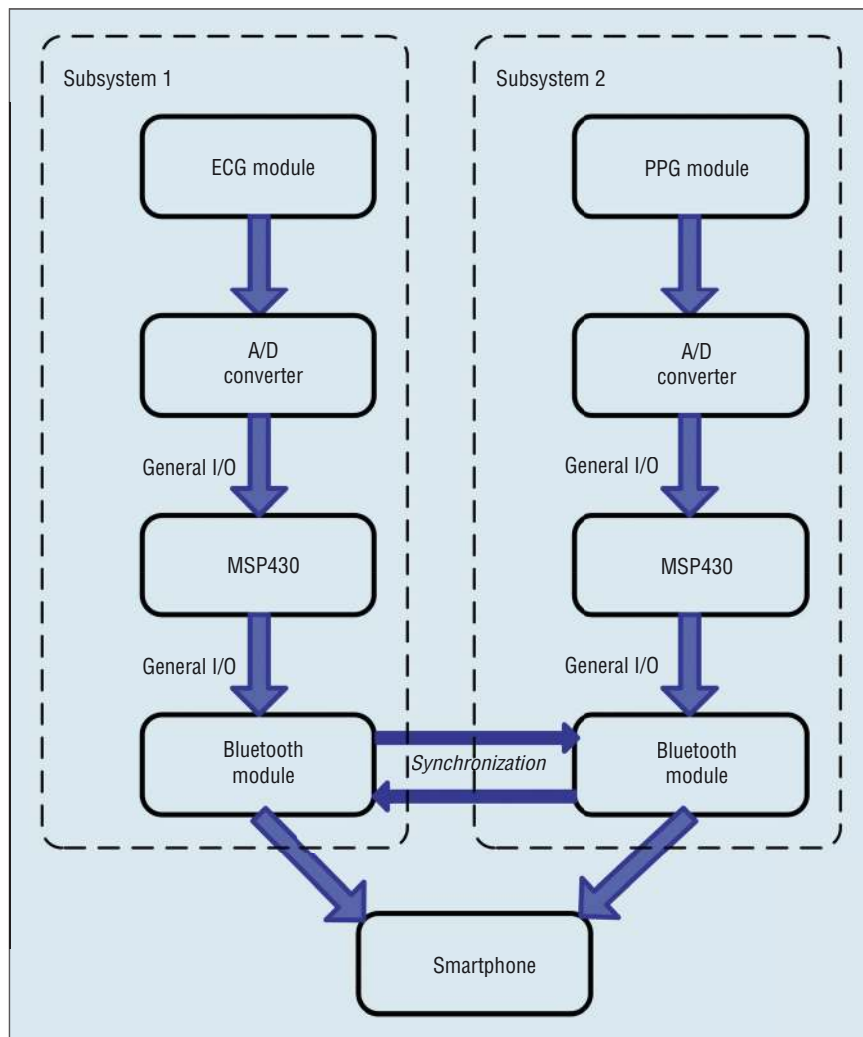

Figure 3. Hardware system. The system consists of seven major components: two MSP430 microprocessor boards, two Bluetooth modules, an ECG module, a PPG module, and an analog-to-digital (A/D) converter.
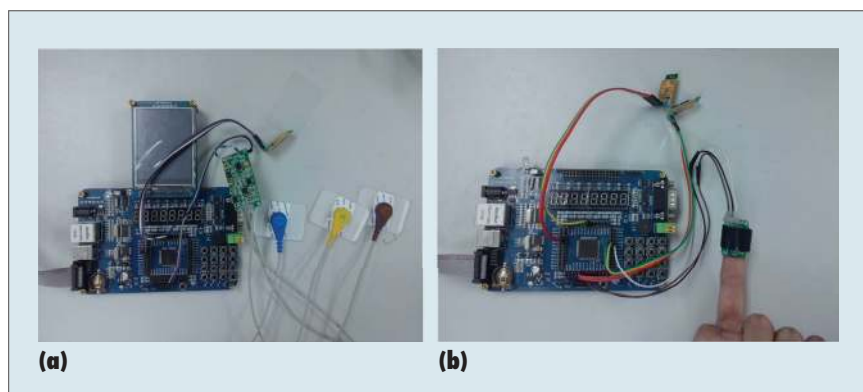

Figure 4. Our prototype hardware platform: (a) ECG subsystem and (b) PPG subsystem. Subsystem 1 collects the ECG signal using an ECG module, and subsystem 2 collects the PPG signal from one finger. Each subsystem is controlled by an MSP430 microprocessor widely used in low-power electronics products.
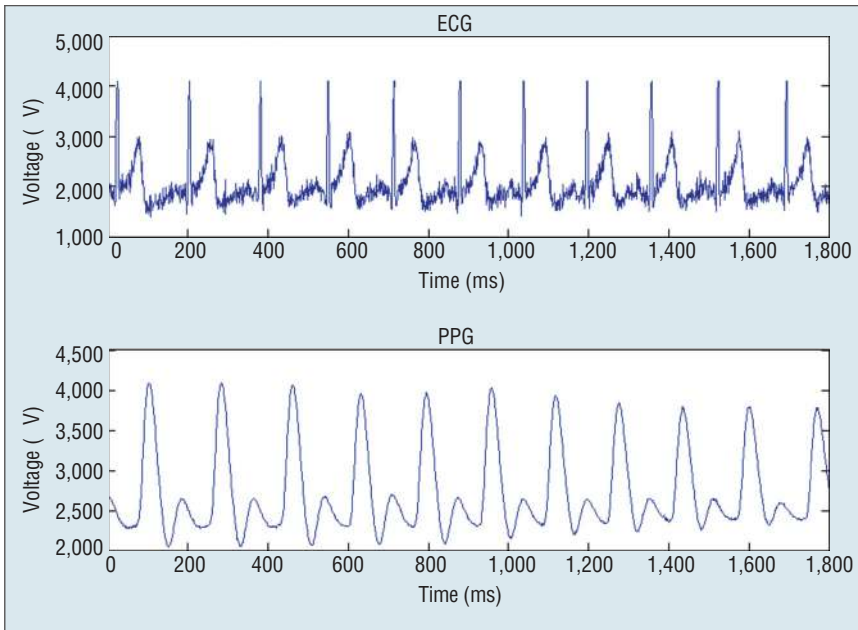
Figure 5. ECG and PPG signals. The two subsystems are synchronized via their Bluetooth modules by transmitting a timestamp to each other; this process repeats after a fixed period. The sampled data are converted into digital signals and uploaded to the smartphone via Bluetooth.
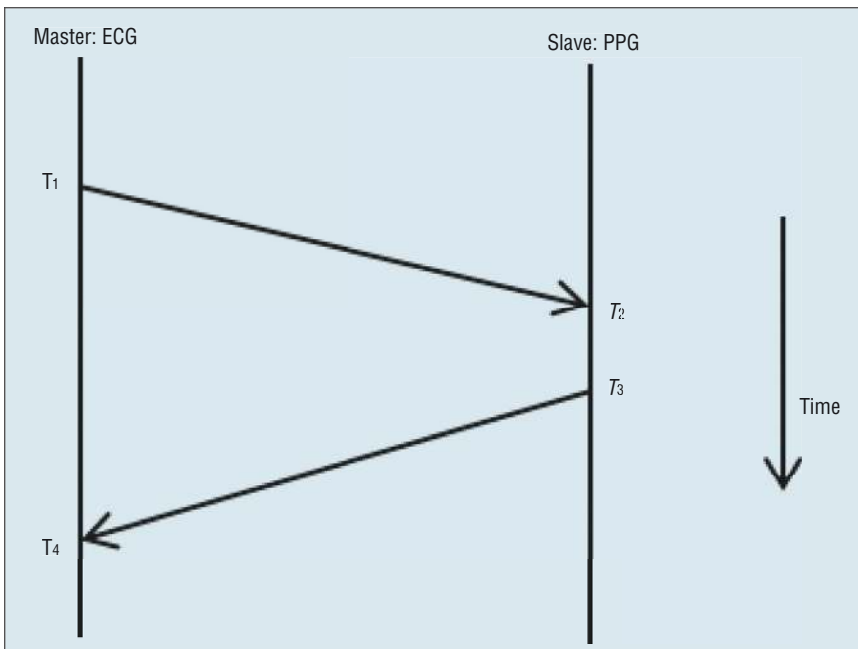

Figure 6. Synchronization between ECG and PPG modules. The ECG subsystem acts as the master, transmitting synchronization messages via Bluetooth to the PPG subsystem. The PPG subsystem receives the message and answers immediately.

timestamp as T_4. Influenced by external factors, the single chip's system clock may generate tiny changes leading to the offset between the two subsystems' changes after a period of time, causing the synchronization procedure to repeat with a fixed time interval.

The system assumes that the timestamp's transmission time between the two subsystems is a fixed value TR. The sum of the offset δ of the two subsystems and the transmission time TR is given by

$$TR + \delta = T_2 - T_1. \tag{1}$$

The offset of the two subsystems subtracting the transmission time is given by

$$TR - \delta = T_4 - T_3. \tag{2}$$

Therefore, the offset between the two devices is calculated by

$$\delta = \frac{(T_2 - T_1) + (T_3 - T_4)}{2}. \tag{3}$$

After calculating the offset δ in Equation 3, the next step is to align the two signals' waveforms. If δ is larger than zero, it means the ECG signal is lagging behind the PPG signal. Otherwise, the ECG signal is ahead of it. Algorithm 1 shows the procedure to align the two waveforms, where δ is counted as the number of sampling periods.

We observe a maximum drift of 1 millisecond between the two clocks per second, so the synchronization procedure is invoked periodically to resolve this drift. There's a tradeoff between the processing capacity and energy consumption on one hand and clock synchronization precision on the other when setting the synchronization period. In all our experiments, we set the synchronization period to 1 second, for which the additional energy consumption and occupied processing capacity can be ignored.

The crystal oscillator of the MPS430 processor used in our system can exhibit frequency drift over temperature. The crystals' standard operation temperature is 25°C, and the drift is about 80 parts per million (PPM) at

```
Require: timestamps T₁, T₂, and T₃; ECG and PPG signals.
Ensure: synchronous ECG and PPG signals
Calculate the offset δ of the two signals in Equation 3.
If δ ≥ then
        Add δ data 0 toward the start of the ECG signal.
Else
      Delete |δ| data from the start of the ECG signal.
end if
```

Algorithm 1. Aligning the two waveforms to synchronize the two subsystems.

–20°C and 10 PPM at 40°C. For this article, we conducted all experiments in an environment with a stable temperature of about 25°C; drift due to temperature change wasn't considered in the software design. To apply our system to realistic living environments with different temperatures, software can improve measurement results by correcting measured values, which we leave as future work.

Another factor affecting clock offset δ estimation is the nondeterministic and nonuniform delay introduced by Bluetooth wireless communication. We performed experiments to evaluate Bluetooth communication delay variance—specifically, we let one MPS430 processor send messages periodically (every 20 milliseconds) to the other MPS430 processor, on which the receiving timestamps are recorded. We observed that variance in the separation of received timestamps was very small (smaller than 0.1 millisecond), and the effect on sampling precision was limited in our prototype system.

PTT and HR Calculation

To estimate PTT and HR, we use the ECG R-wave and PPG peak as feature points. Specifically, we use the method described elsewhere (www.librow.com/cases/case-2) to detect ECG and PPG peaks, which includes two steps:

- To remove the baseline drift and balance the baseline, we apply a fast Fourier transform to the original ECG signals, and the waveform is restored through inverse transformation.
- To identify peaks, we apply a window function to the waveform, leading to the discovery of one window's maximum value. A predefined threshold removes any meaningless points.
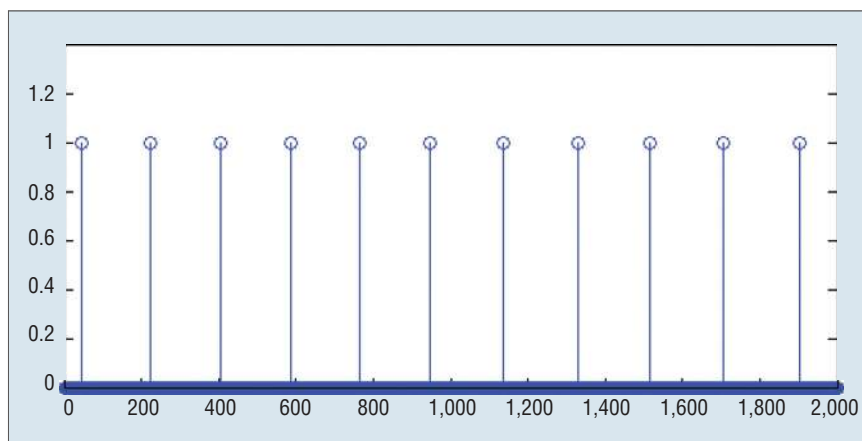

Figure 7. Determination of peak ECG signal. Pulse transit time (PTT) is usually determined by the ECG R-wave and the pulse wave's arrival determined by the PPG's peak value.

Figure 7 shows the result of peak detection for ECG signals. Note that the thresholds in our system are fixed; adaptive thresholds might be useful to improve detection quality in realistic environments, which we leave as future work.

Using the same method applied to the ECG signal, we can detect PPG signal peaks:

$$HR = \frac{60}{W_t} \times n, \qquad (4)$$

where n is the number of PPG signal peaks within a time window of length W_t (in seconds).

PTT is usually determined by the ECG R-wave and the pulse wave's arrival determined by the PPG's peak value, as Figure 8 shows. The ECG's R-wave represents each heartbeat's start time, but there's a delay between the start time and blood ejection from the heart when intracardiac force exceeds the force out of the heart. This delay—the pre-ejection period (PEP)—makes the measured PTT greater than the true PTT (denoted by tPTT). So the measured PTT consists of two parts:

$$PTT = PEP + tPTT. \qquad (5)$$

The difference between PTT and tPTT is an important reason why existing methods are so imprecise in estimating BP via PTT measurements.
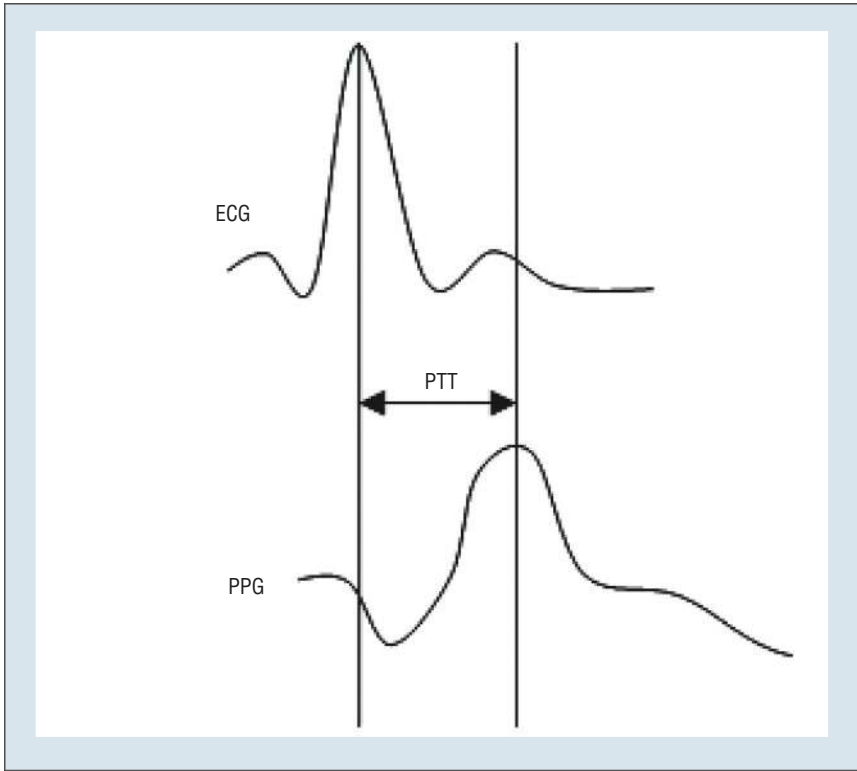
Figure 8. PTT determined by the ECG and PPG.

Table 1. Subject information.

Subjects	Height (cm)	Amount of data	Age
Subject1	176	50	24
Subject2	170	50	23
Subject3	165	50	25
Subject4	160	50	24
Subject5	170	50	24
Subject6	163	50	22

BP Estimation with Baroreflex

The baroreflex mechanism regulates BP changes, so we developed a PTT-based model that considers this mechanism.

Baroreflex. The arterial baroreflex, a basic mechanism for the short-term regulation of BP, plays an important role in maintaining BP at nearly constant levels. The regulatory process is based on neuroregulation: arterial baroreceptors provide the central nervous system with continuous information on BP, with changes sensed by stretch receptors in the walls of the carotid sinuses and aortic arch. When systemic arterial pressure rises, the arterial baroreceptors are activated, leading to a phenomenon where the discharging of vagal cardioinhibitory neurons increases and the discharging of sympathetic neurons decreases.

These phenomena result in bradycardia, decreased cardiac contractility, decreased peripheral vascular resistance, and venous return. Conversely, decreased systemic arterial pressure leads to deactivation of baroreceptors, which enhances the sympathetic activity and inhibits the vagal. These result in tachycardia, increased cardiac contractility, increased vascular resistance, and venous return. Experiments also show that an impairment of baroreflex mechanisms can reflect cardiovascular diseases—for example, a reduction in HR baroreflex control has been reported in hypertension, coronary artery disease myocardial infarction, and heart failure.[8]

PTT-based baroreflex model. According to the principle of energy conversion, the work from force can convert into a wave's kinetic energy and gravitational potential energy when a pulse wave travels from the heart to the fingertip. Other researchers[9] calculated BP by using the following formula:

$$BP = \frac{A}{PTT^2} + B, \qquad (6)$$

where A is related to the subject's height,

$$A = (0.6 \times height)^2 \times \frac{\rho}{1.4}, \qquad (7)$$

and ρ = 1,035 kg/m^3 is the average blood density.

The model in Equation 6 assumes an ideal condition, in which the artery is a rigid pipe when laminar blood flows from the heart chamber to the fingertip, thus the PEP is included in the PTT, making it longer than the tPTT we discussed earlier.

The effect of arterial baroreflex is to adjust the short-term regulation of BP and prevent wide fluctuations. HR plays a main role here, and the baroreflex can reflect the relationship between BP and HR: to adjust BP to a stable state, HR decreases when BP increases, and vice versa. Because of the rapidity of vagal response, BP has been shown to have a proportional relationship with respect to
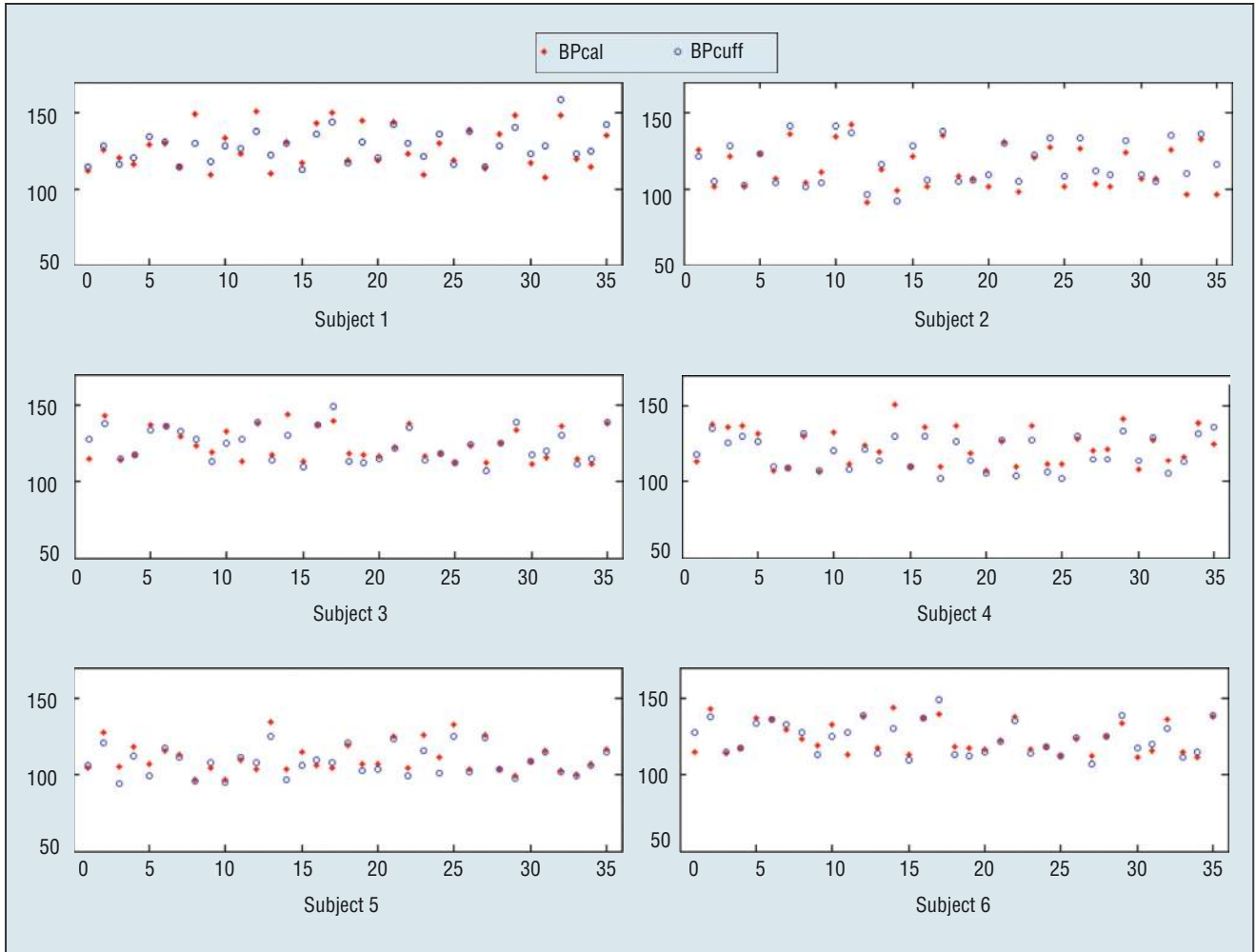
Figure 9. BP values measured by sphygmomanometer (BPcuff) and BP calculated from the PTT (BPcal) of six subjects. BPcal tracks BPcuff with good precision.

R-R interval, which is inverse to HR. Baroreflex sensitivity is defined as the ratio between the change in the R-R interval and the change in BP.[8] Considering arterial baroreflex, we propose a new formula for BP estimation consisting of a PTT part introduced in Equation 6 and a new part reflecting HR's influence:

$$BP = \frac{A}{PTT^2} + \frac{C}{HR^2} + D, \qquad (8)$$

where A is still calculated according to Equation 7, and other parameters are estimated by least square fitting.[8]

The function consists of two variables, PTT and HR, which make the formula expressing a 3D model and HR is an additional item to adjust the BP estimation. Note that our model is different from one presented elsewhere[10] that assumes a proportional relation between HR and BP. That model is based on the observation that, for example, after doing exercise, a subject's HR and BP both increase. However, a closer look into the baroreflex mechanism shows that an inverse relation between HR and BP should be used to correctly adjust the BP estimation and reflect the baroreflex mechanism in the (dominating) proportional relation between PTT and BP.

Experimental Results

We verified our new BP model in Equation 8 with 300 groups of data from six healthy subjects collected under indoor conditions. We divided the data for each subject into two parts: part 1 (30 percent) to construct the models and part 2 (70 percent) for evaluation. Table 1 shows the information for every subject, and the measurement process was as follows:

- The subjects were asked to relax for several minutes in a sitting position, and then the ECG and PPG signals were recorded for 1 minute with the hardware system
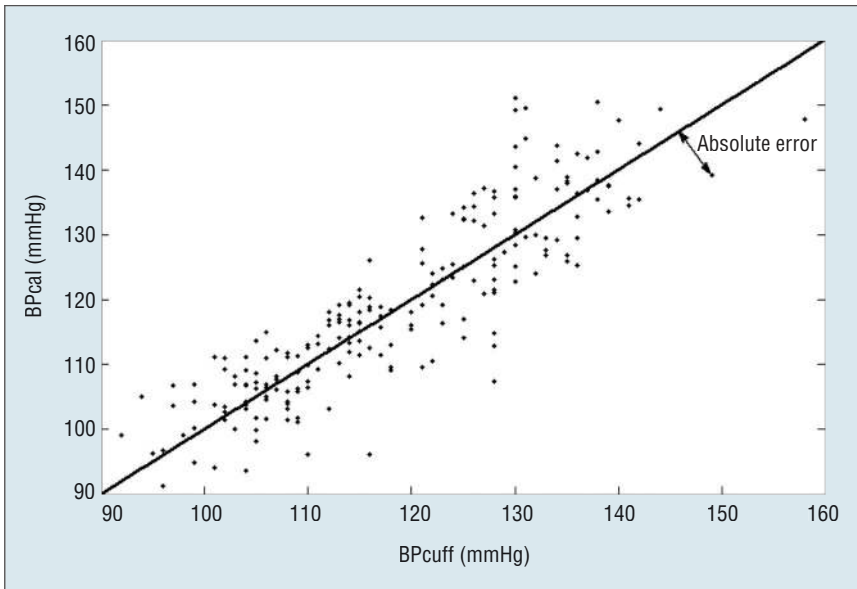
Figure 10. Scatter plots of BP measured by a sphygmomanometer (BPcuff) and BP calculated from PTT (BPcal). The straight line represents the diagonal, which means that BPcuff equals BPcal. The distance between the points and the diagonal represents the absolute error of BPcal against BPcuff.
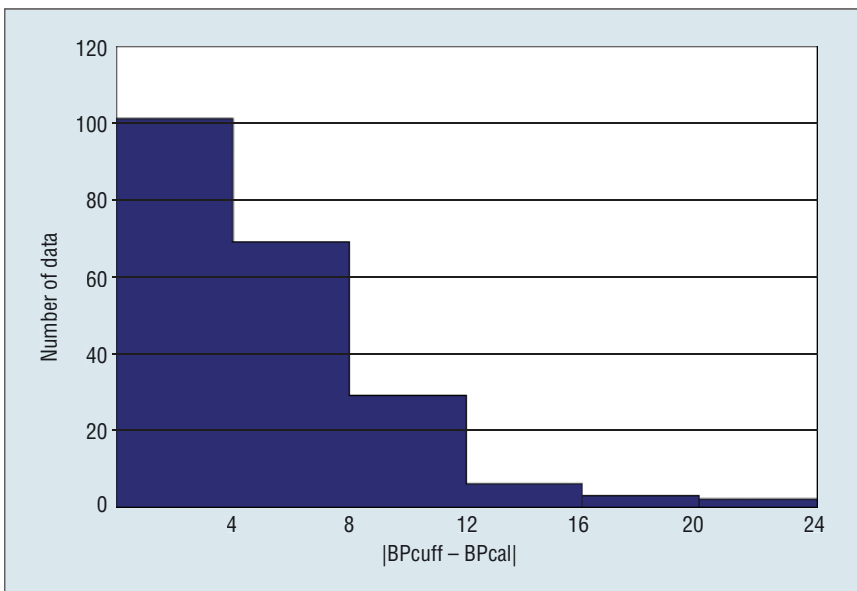

Figure 11. Histogram of the relative error. Most of the data are less than 6 percent and only a few are more than 12 percent.

presented earlier. We used the numerical average of the calculated BP values using Equation 8 within 1 minute for BP estimation, denoted by BPcal. We also measured each subject's BP with the sphygmomanometer on the same hand,

the result of which is denoted by BPcuff.

• Subjects were then asked to do exercises for several minutes, after which another group of data was collected immediately using the method just described.

• We repeated the process 25 times for every subject.

Evaluating Accuracy

The processing procedure for every subject was as follows. We first estimated the parameter using the least square method and established the BP function with different parameters for different subjects. Then, based on the function for each subject, we estimated BP (BPcal) using PTT and HR according to Equation 8 and compared it with BP measured by a sphygmomanometer (BPcuff). Note that we trained the model for each subject individually: we tested the models on the same data on which they were evaluated, and we didn't consider real-time model adjustment or recalibration.

Figure 9 shows the BPcuff and BPcal values for different subjects, where we can see that BPcal tracks BPcuff with good precision. Figure 10 shows the scatter plot of BPcal versus BPcuff; the straight line represents the diagonal, which means that BPcuff equals BPcal. The distance between the points and the diagonal represents the absolute error of BPcal against BPcuff. Figure 11 shows the histogram of the relative error, where most of the data are less than 6 percent and only a few are more than 12 percent.

Table 2 summarizes the maximal absolute error, minimal absolute error, and average absolute error by using our method in Equation 8 and in Equation 6.[9] Our method can improve the precision by about 10 percent.

Evaluating Robustness

Figure 12 shows the Bland-Altman plot of the BP data to compare the relative error of our model and that of Fung's team.[9] The mean represents the

Table 2. Comparing our method with that of Parry Fung and colleagues.[9]

Subjects	Method	Maximal error	Minimal error	Average error	Standard deviation
1	Ours	16.7655	0.0620	4.7619	5.8258
	Fung's	22.4263	0.1880	5.7665	7.4696
2	Ours	20.6702	0.1199	5.3408	7.0343
	Fung's	25.6233	0.1860	6.3550	8.3279
3	Ours	16.1049	0.1721	5.0351	6.1206
	Fung's	19.2354	0.1564	5.2152	6.4858
4	Ours	15.9468	0.0374	3.7841	5.1598
	Fung's	14.4904	0.1469	4.0378	5.4320
5	Ours	17.5500	0.0602	4.2605	5.5634
	Fung's	17.3753	0.1310	4.4228	5.8652
6	Ours	8.8835	0.0202	3.6123	4.4367
	Fung's	8.6735	0.1507	3.6401	4.4474
Average	Ours	15.9868	0.0786	4.4658	5.6901
	Fung's	17.9707	0.1598	4.9062	6.3380

average of all differences calculated by (BPcuff – BPcal)/BPcuff. We can see that 12 of all pairs of data are located beyond the agreement limits (mean +/2 SD) in Figure 12a (our model) and 14 in Figure 12b (Fung's model), where SD is the standard deviation of the (BPcuff – BPcal)/BPcuff value over all data samples. Our proposed method's SD is 0.4884; it's 0.7486 for Fung's method. This result shows that the data using our model are more concentrated and the error is limited to +/0.0934. Our proposed method's SD is 6.492; it's 7.156 for Fung's method. Figure 13 shows the number of data exceeding different thresholds of the |BPcuff – BPcal| value.

We can improve our method's precision by recalibrating it. Note that each subject's data were collected on different days. BP characteristics can slightly vary on different days, so daily recalibration could greatly improve estimation accuracy. Recalibration might also be required based on normal and high BP values. Therefore, an important aspect for future work is to design, implement, and evaluate our system's recalibration mechanisms. Moreover, we'll expand access to our system, inviting participants with different health conditions—
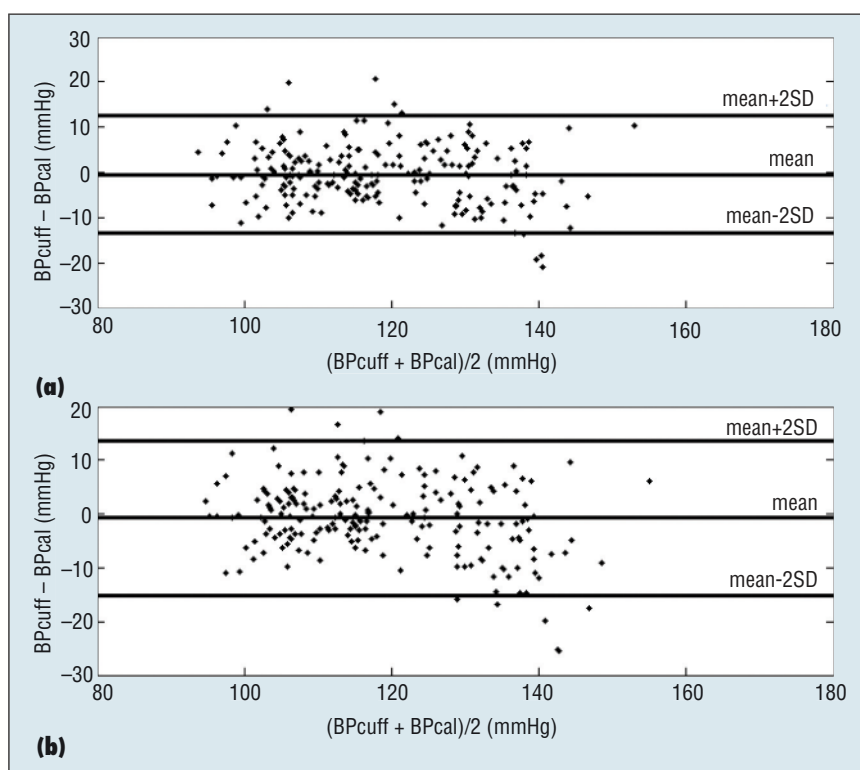

Figure 12. Bland-Altman plot: BP estimation using (a) our method and (b) that of Fung and colleagues.[9] SD is the standard deviation of the (BPcuff – BPcal)/BPcuff value over all data samples. The SD of our proposed method is 0.4884; it's 0.7486 for Fung's method.

for example, those suffering hypertenstion or stiff arteries. ▬

References

1. R.S. Vasan et al., "Assessment of Frequency of Progression to Hypertension in Non-Hypertensive Participants in the
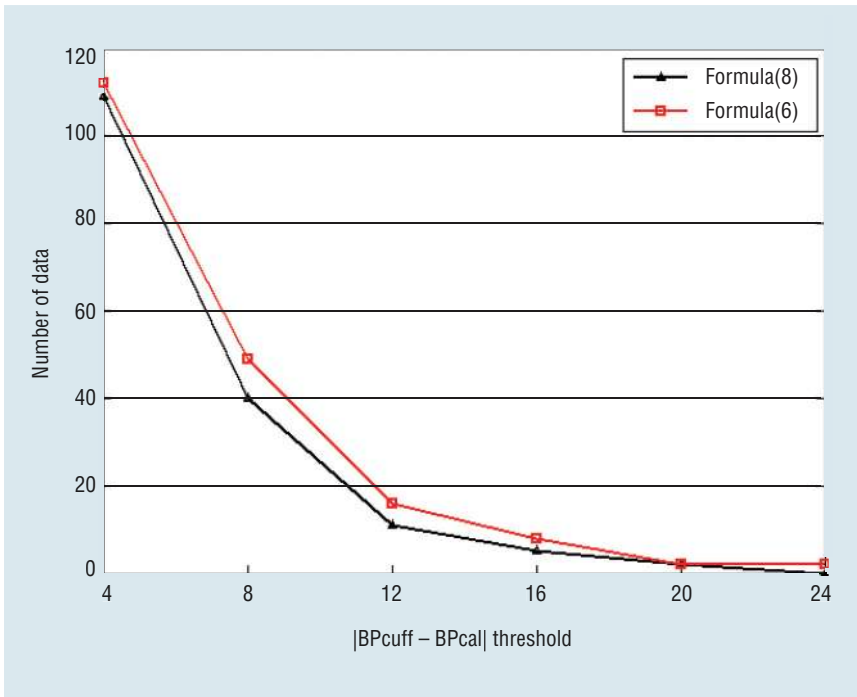
Figure 13. Data under different error thresholds.

THE AUTHORS

Hao Lin is an MS student in the Department of Computer Science and Engineering at Northeastern University, China. His research interests include embedded systems and signal processing. Contact him at linhao.neu@gmail.com.

Wenyao Xu is an assistant professor in the Department of Computer Science and Engineering at the State University of New York (SUNY), Buffalo. His research interests include embedded systems, computer architecture, compressed sensing, and machine learning. Xu received a PhD in electrical engineering from the University of California, Los Angeles. He's a member of IEEE. Contact him at wenyaoxu@buffalo.edu.

Nan Guan (the corresponding author) is a full professor in the Department of Computer Science and Engineering at Northeastern University, China. His research interests include cyber-physical systems, real-time scheduling theory, and program analysis. He's a member of IEEE. Contact him at guannan@ise.neu.edu.cn.

Dong Ji is a PhD student in the Department of Computer Science and Engineering at Northeastern University, China. His research interests include embedded systems, new energy vehicles, and signal processing. Contact him at jidong893@gmail.com.

Yangjie Wei is an associate professor in the Department of Computer Science and Engineering at Northeastern University, China. Her research interests are in micro/nano observation, 3D reconstruction, and micro/nano image processing. Wei received a PhD in recognition and intelligent systems from the Shenyang Institute of Automation, Chinese Academy of Science. Contact her at weiyangjie@ise.neu.edu.cn.

Wang Yi is a full professor at Northeastern University, China. He's also the chair of the embedded systems department at Uppsala University, Sweden. His research interests include models, algorithms, and software tools for modeling and verification, timing analysis, and real-time scheduling. Yi received a PhD in computer science from Chalmers University of Technology. He's a fellow of IEEE. Contact him at yi@it.uu.se.

Framingham Heart Study: A Cohort Study," *The Lancet*, vol. 358, no. 9294, 2001, pp. 1682–1686.

2. V. Chandrasekaran et al., "Cuffless Differential Blood Pressure Estimation Using Smart Phones," *IEEE Trans. Biomedical Eng.*, vol. 60, no. 4, 2013, pp. 1080–1089.

3. R.P. Smith et al., "Pulse Transit Time: An Appraisal of Potential Clinical Applications," *Thorax*, vol. 54, no. 5, 1999, pp. 452–457.

4. M.Y.M. Wong, E. Pickwell-MacPherson, and Y.T. Zhang, "The Acute Effects of Running on Blood Pressure Estimation Using Pulse Transit Time in Normotensive Subjects," *European J. Applied Physiology*, vol. 107, no. 2, 2009, pp. 169–175.

5. J. Muehlsteff, X.L. Aubert, and M. Schuett, "Cuffless Estimation of Systolic Blood Pressure for Short Effort Bicycle Tests: The Prominent Role of the Pre-Ejection Period," *Proc. Int'l Conf. Eng. Medicine and Biology Soc.*, 2006, pp. 5088–5092.

6. M.J. Drinnan, J. Allen, and A. Murray, "Relation between Heart Rate and Pulse Transit Time during Paced Respiration," *Physiological Measurement*, vol. 22, no. 3, 2001, p. 425.

7. P.M.P. da Silva, "A Pervasive System for Real-Time Blood Pressure Monitoring," master's thesis, Dept. of Eng., Univ. of Porto, 2013; http://paginas.fe.up.pt/~ee08234/dissertacao/index.html.

8. M.T. La Rovere, G.D. Pinna, and G. Raczak, "Baroreflex Sensitivity: Measurement and Clinical Implications," *Annals of Noninvasive Electrocardiology*, vol. 13, no. 2, 2008, pp. 191–192.

9. P. Fung et al., "Continuous Noninvasive Blood Pressure Measurement by Pulse Transit Time," *Proc. 26th Ann. Int'l Conf. Eng. Medicine and Biology Soc.*, 2004, pp. 738–741.

10. S. Mottaghi, M.H. Moradi, and L. Roohisefat, "Cuffless Blood Pressure Estimation during Exercise Stress Test," *Int'l J. Bioscience, Biochemistry and Bioinformation*, vol. 2, no. 6, 2012, pp. 394–397.